Chemical Science

RSC Publishing

Chemical Science

RSC Publishing

MINIREVIEW

Amplifications in chiroptical spectroscopy, optical enantioselectivity, and weak value measurement

Cite this: *Chem. Sci.*, 2013, **4**, 4107

Hanju Rhee,[a] Joseph S. Choi,[b] David J. Starling,[c] John C. Howell[d] and Minhaeng Cho*[ae]

Received 7th May 2013
Accepted 22nd July 2013

DOI: 10.1039/c3sc51255j

www.rsc.org/chemicalscience

Chiroptical spectroscopy utilizing left- and right-handed electromagnetic fields has been used to obtain stereochemical information on chiral molecules in condensed phases. However, due to weak signals (10^{-6} to 10^{-2} of absorption), not only are accurate measurements of chiroptical signals difficult but also preferential excitation of one type of handed molecule over the other using chiral fields (*i.e.*, optical enantioselectivity) is limited. Recently, methods have been developed to enhance chiroptical signals and optical enantioselectivity by properly controlling polarization states, designing detection schemes, and modifying spatial properties of chiral fields. In the physics community, similar enhancements have been introduced using a quantum mechanical theory called "weak value measurement." Here we provide examples of these techniques, corresponding enhancement mechanisms, and more importantly connections between them.

Introduction

Chirality, from the Greek word meaning 'hand', is a property of left- or right-handedness of geometries that have a non-superposable mirror image. Similar to chiral recognition (*e.g.* shaking hands, turning screws) usually encountered in the macroscopic world, the relevant phenomena at the submicroscopic scale also show intriguing structure-specific aspects, leading to diverse research interests. In particular, molecular chirality plays a vital role in a variety of chemical and biological processes including asymmetric synthesis, enzyme catalysis, ligand binding to biomolecules, *etc.* Naturally, its characterization is essential for understanding the underlying mechanisms, functions and dynamics of those molecular systems.[1,2]

Chiroptical spectroscopy[3,4] is a decisive tool to characterize molecular chirality in a simple way by measuring the difference of optical signals induced by left- and right-circularly polarized (LCP and RCP) light. The chiroptical spectroscopic method has been used extensively and complementarily for investigating structural properties of chiral molecules in condensed phases. The simplicity and easy accessibility of the method has often precluded other high precision techniques offering atomic resolution structure such as 2D-NMR and X-ray diffraction. Relevant applications now continue to grow, which include characterizations of chiral nanomaterials, supramolecules, biopolymers, catalysts, medical drugs, *etc.* with various types of linear chiroptical methods[5–7] such as circular dichroism (CD), optical rotatory dispersion (ORD), and Raman optical activity (ROA).[3,4]

Chiral signals are intrinsically very weak (10^{-6} to 10^{-2} of absorption) so that accurate measurements can be challenging. Such is the case for low concentration experiments with biosamples or fast time-resolved studies probing subtle pump-induced changes in molecular chirality, much smaller than the corresponding equilibrium signal. In this regard, signal enhancement-and-amplification in chiroptical spectroscopy is an important step toward its successful application; such an application will help to elucidate many concealed biochemical processes involving molecular chirality changes.

A practical application of chiral field and chiral molecule interactions can be realized with optical enantioselectivity. Optical enantioselectivity is the photo-selection of one form of optical isomer over the other in a racemic mixture (containing left and right-handed molecules in equal amounts). Typically, circularly polarized light is used, in which case the differential absorption is called circular dichroism (CD). Recently, attempts have been made to improve upon the typical CD measurements by engineering the fields or the detection schemes used.

A highly accurate measurement of weak physical effects, similar to chiroptical phenomena, has been a problem for experimentalists in all fields of science. In physics, recent high precision experiments have demonstrated measurements of 1 Å displacements[8] and 400 femtoradian deflections.[9] These developments stemmed from a quantum mechanical "weak value"

[a]*Division of Analytical Research, Korea Basic Science Institute, Seoul 136-713, Korea*
[b]*The Institute of Optics, University of Rochester, Rochester, New York 14627, USA*
[c]*Division of Science, Pennsylvania State University, Hazleton, Pennsylvania 18202, USA*
[d]*Department of Physics and Astronomy, University of Rochester, Rochester, New York 14620, USA*
[e]*Department of Chemistry, Korea University, Seoul 136-713, Korea. E-mail: mcho@korea.ac.kr; Fax: +82-2-3290-3121; Tel: +82-2-3290-3133*

theory on measurements by Aharonov, Albert and Vaidman (AAV) proposed in 1988.[10] Counter-intuitively, the AAV theory requires the coupling of the measurement device 'meter' and system states to be weak. This theory can be used[11] to explain the chiroptical signal enhancements shown by Kliger's group in 1985,[12] and more recently by the Cho group.[13–15]

Background: molecular chirality and optical chirality

A molecule is called 'chiral' when it does not coincide with its mirror image like an amino acid with four different groups around a central carbon (dissymmetry center). The opposite mirror image enantiomers, whose absolute configurations are usually specified by (*R*) and (*S*) designations, look similar to each other but have different chemical properties. Complex macromolecules such as proteins and DNA also create highly rigid and twisted chiral parts of the backbone through specific long-range interactions such as hydrogen-bonds.

The structural dissymmetry of such chiral molecules causes a phenomenon known as optical activity, represented by the differential interaction of matter with two optically chiral (left and right) circularly polarized beams. When the oscillating electric field of light interacts with a chiral molecule having an asymmetric distribution of charges, both linear and angular components of charge oscillation (their combined motion is helical!) are produced, which in turn induce transition electric ($\boldsymbol{\mu}$) and magnetic ($\boldsymbol{m}$) dipoles, respectively. The radiation–matter interaction Hamiltonian (H_I) can thus be written as:[16]

$$H_I = H_E + H_B + \ldots = -\boldsymbol{\mu}\cdot\boldsymbol{E} - \boldsymbol{m}\cdot\boldsymbol{B} + \ldots \quad (1)$$

where $\boldsymbol{E}$ and $\boldsymbol{B}$ are the electric and magnetic fields of light. The first term, H_E (electric dipole–electric field interaction), is associated with the conventional electric dipole-allowed transition and light absorption. The second term, H_B (magnetic dipole–magnetic field interaction), leads to linear optical activity, when it is combined with the first term in eqn (1). The absorption and optical activity are proportional to dipole ($DS = |\boldsymbol{\mu}|^2$) and rotatory ($RS = \mathrm{Im}[\boldsymbol{\mu}\cdot\boldsymbol{m}]$) strengths, respectively. The former provides information only on the absorption intensity, whereas the latter adds the phase (peak sign) determined by the relative orientation of $\boldsymbol{\mu}$ and $\boldsymbol{m}$ in a given molecule. The latter is the reason why chiroptical spectroscopy is sensitive to chiral molecular structures and therefore of use in differentiating them.

In addition to "molecular chirality", one can define "optical chirality" as (see ref. 17):

$$C \equiv \frac{\varepsilon_0}{2}\boldsymbol{E}\cdot\nabla\times\boldsymbol{E} + \frac{1}{2\mu_0}\boldsymbol{B}\cdot\nabla\times\boldsymbol{B} \quad (2)$$

to quantify the degree of chirality for an arbitrary electromagnetic (EM) field in vacuum. This can be easily generalized for EM fields in materials by replacing the vacuum permittivity and permeability with their general values. For the generalized *C*, the field becomes coupled to the material properties, and is time-invariant for monochromatic fields.[18]

The optical chirality is the same as the "Z^{000} Zilch" defined by Lipkin in 1964.[19] This and other "zilches" are conserved quantities in vacuum, but were dismissed as physically irrelevant by Lipkin and colleagues at the time.[19,20] Others have since interpreted Lipkin's zilches to represent the "angular momentum" of the curl of the electromagnetic field.[21] They stated that a "helicity density," not optical chirality, is what actually has dimensions of angular momentum per unit volume, considering "optical chirality" to be an inappropriate term. However, for monochromatic fields, helicity densities and zilches are proportional to each other by the square of the angular frequency. Therefore, the optical chirality in eqn (2) is physically proportional to the angular momentum density of the EM fields.

Chiroptical spectroscopy: intensity *versus* phase-amplitude measurements

Conventional chiroptical approaches are based on intensity measurements with LCP(+) and RCP(−) beams, in which weak ± phase signals can be obtained by taking the difference of their intensities ($I_\pm$). In CD spectroscopy, the chiral signal (*s*) is given by the intensity difference normalized by the mean intensity:

$$s = \frac{I_+ - I_-}{(I_+ + I_-)/2} \quad (3)$$

In general, eqn (3) is used both in absorption (CD) and emission methods, where the latter includes chiral luminescence, ROA, and so on. In this minireview, however, our discussion will be focused on the absorption process so that $I_\pm$ is restricted only to the transmitted field intensity. Here the ± sign indicates opposite polarization beams that are mirror images to each other, *e.g.*, LCP and RCP light, left- and right-elliptically polarized light, or (+)- and (−)-rotated linearly polarized (LP) light, for CD or ORD measurements, respectively. In a real measurement, however, this intensity differential measurement is unfavorable for differentiating a weak chiral signal masked by a huge achiral background noise; that is, light intensity fluctuations usually overwhelm such a weak chiroptical effect ($s \sim 10^{-5}$), significantly deteriorating the measurement sensitivity.

The ellipsometric approach[3,22] pioneered by Kliger is one way to amplify the signal-to-noise ratio (SNR). Here, left- and right-elliptically polarized (LEP and REP) light rather than circular is used in combination with polarizers allowing only a transmission of the minor-axis field of the elliptically polarized (EP) light. This type of measurement is referred to as self-heterodyne because a signal induced by the incident radiation self-interferes with the incident radiation itself, where the minor-axis field of EP light acts as a local oscillator (LO). By controlling the ellipticity of the EP light, *i.e.*, LO amplitude, one can effectively remove most of the background contribution without loss of the chiral signal. The differential ellipsometric technique with both LEP and REP light has been used to measure fast time-resolved electronic CD[22] and very weak vibrational CD signals[23] in the UV to IR frequency range. Recently, we have developed an alternative self-heterodyne detection method[13,15,24] (Fig. 1a) requiring no polarization switching between LEP and REP. This enables

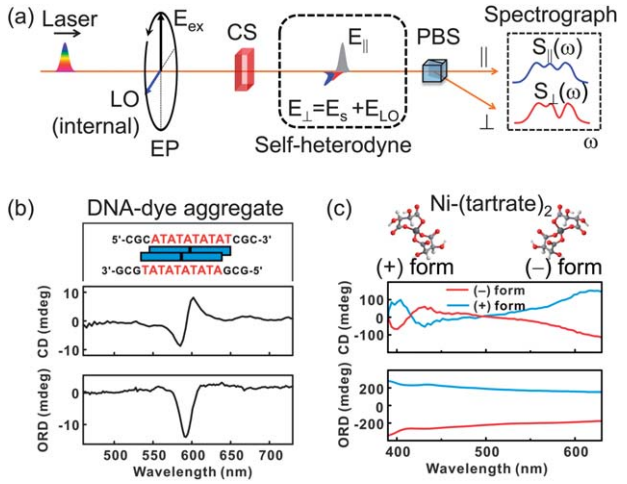

Fig. 1 (a) Self-heterodyne CD measurement scheme. EP: elliptical polarization; CS: chiral sample; PBS: polarizing beam splitter. CD/ORD spectra of (b) DNA–cyanine dye complex and (c) (±)-Ni-(tartrate)$_2$ measured with self-heterodyne measurement techniques based on the scheme in (a). Note that the ORD spectra were measured by using a rotated LP beam instead of the EP in (a).

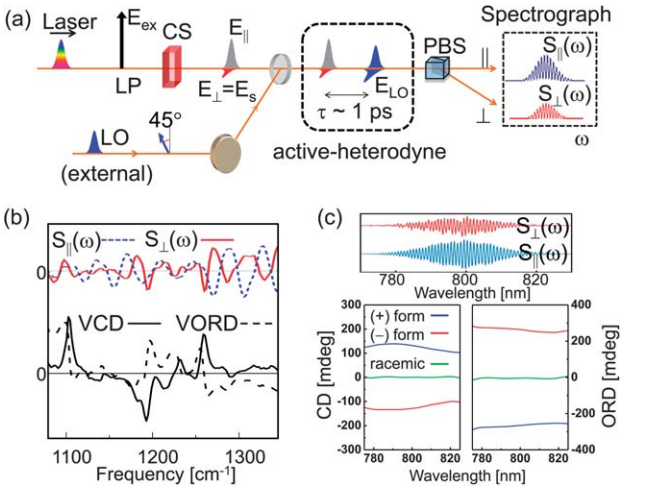

Fig. 2 (a) Active-heterodyne OA FID measurement scheme. LP: linear polarization; CS: chiral sample; PBS: polarizing beam splitter. (b) Vibrational CD/ORD (VCD/VORD) spectra of C–C stretching modes of (1*S*)-β-pinene and (c) near-IR electronic CD/ORD spectra of (±)-Ni-(tartrate)$_2$ and their racemic mixture, obtained from parallel- ($S_{\parallel}(\omega)$) and perpendicular-detected ($S_{\perp}(\omega)$) spectral interferograms measured by using active-heterodyne measurement techniques shown in (a).

direct characterization of the chiral signal (*s*) with just a single polarization state. This is therefore known as a non-differential measurement technique. It was demonstrated that broadband CD/ORD measurements with a super-continuum pulse are achievable in a shot-by-shot basis. Fig. 1b and c show UV-visible electronic CD/ORD spectra of chiral DNA–dye aggregates and organometallic ((±)-Ni-(tartrate)$_2$) compounds measured using this method, respectively.[24]

The wave interference method,[13,15,25] a recent remarkable achievement in chiroptical spectroscopy, is another choice to enhance the chiroptical measurement sensitivity. It can be used to directly characterize the phase and amplitude of an optical activity free-induction decay (OA FID) field. In contrast to the self-heterodyne measurement utilizing an internal LO from the incident beam, another external LO is used. This LO, whose properties can be separately controlled (active-heterodyne), is used to interfere with the OA FID to generate an interferogram in the frequency domain (Fig. 2a). With a well-known Fourier transform procedure,[26] both CD and ORD spectra can simultaneously be retrieved from parallel- and perpendicular-detected spectral interferograms. Shown in Fig. 2b and c are examples measured in the mid- (vibrational CD/ORD) and near-IR (electronic CD/ORD) frequency range. Unlike the ellipsometric method requiring precise control of the incident polarization state (ellipticity), the signal enhancement can easily be achieved by controlling the external LO intensity with an optical attenuator.

Optical enantioselectivity: travelling *versus* standing waves

A metric appropriate for measuring the enantioselectivity of a system is given by a modified form of the dimensionless dissymmetry factor. First proposed by Kuhn using the decadic molar extinction coefficient, the dissymmetry factor can be described as the ratio of CD to conventional absorption. The dissymmetry factor is then a proper criterion, given the available instrumental sensitivity, for determining whether the CD is measurable for a particular absorption band.[27] To determine the degree of optical enantioselectivity, the following dissymmetry factor *g* was considered,[17] which is essentially the same as Kuhn's:

$$g = \frac{A^+ - A^-}{(A^+ + A^-)/2} \leq 2 \qquad (4)$$

Here, $A^{\pm}$ is the absorbance for left (+)- or right (−)-handed fields. This is a good measure of optical enantioselectivity since it measures the differential absorbance of the chiral molecules related to the average total absorbance.

When using LCP and RCP light, which is how CD and ORD measurements are made, the dissymmetry factor is proportional to the rotatory strength *RS* over the dipole strength *DS* of the sample.[27] We denote this as g_{CPL}. Since g_{CPL} is typically quite small (10^{-3} to 10^{-2} for electronic excitation and 10^{-6} to 10^{-4} for vibrational excitation), developing methods to increase the dissymmetry factor continues to be a goal of researchers.

Recently, the Cohen group investigated the possibility of using EM fields other than LCP and RCP light to improve optical enantioselectivity.[28] Their original idea was to engineer special EM fields, and thereby enhance optical enantioselectivity. They provided an interesting method to do so, simply by reflecting the incident CPL to create a standing-wave-type chiral field (SWCF). The field was then termed "superchiral" due to the enhancement effect. By creating a standing-wave field (instead of the typical CPL fields) and suppressing the electric field energy density, they were able to experimentally demonstrate an 11× enhancement over g_{CPL} (see Fig. 3).

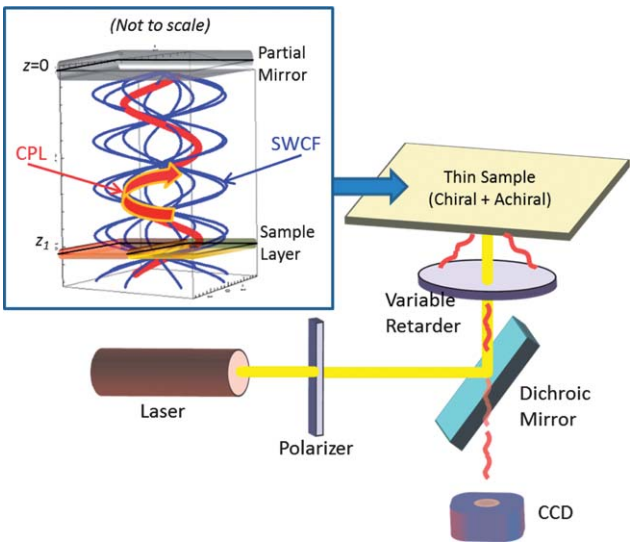

Fig. 3 Experimental setup for measuring enhanced optical enantioselectivity using a standing-wave-type chiral field (SWCF).[28] Two samples are used, one with mirror coating, and one without, to measure g and g_{CPL}, respectively. The thin sample has both a chiral and an achiral layer on a 170 μm thick glass coverslip. Laser light is polarized to avoid distortion from the dichroic. The variable retarder converts the linearly polarized light alternately into left- and right-circularly polarized light. Fluorescence is imaged on a charge-coupled device (CCD), after being separated from excitation light by the dichroic mirror and a filter (not shown). (Inset) electric fields of SWCF compared to circularly polarized light (CPL) interacting with the chiral/achiral layer ("sample layer"), obtained from the experimental values ($R = 0.72$, 543.5 nm wavelength). The CPL (red) is left-CPL, traveling in the $-z$ direction. When reflected by the mirror, a standing wave (SWCF; blue) is created. The CPL shown is for a fixed time, but the SWCF shown is a sum of eight 1/8 periods. The fields shown are over a propagation distance of ~1.2 μm ($z_1 = 1$ μm). This illustrates that the chiral/achiral sample layer can spatially fit inside a nodal electric field region for the SWCF. (The mirror and sample layer were 19 nm, 10 nm thick, respectively.)

Underlying enhancement mechanisms

In chiroptical spectroscopy, the interference between a weak signal field and an internal (self-heterodyne) or external (active-heterodyne) reference field (LO) is detected. Controlling the LO intensity allows one to make significant enhancements and amplifications of the detected chiral signal field. Fig. 4 shows the basic concept underlying the enhancement mechanism in chiroptical spectroscopy. An LP light, the sum of 50 : 50 co-propagating LCP and RCP light, is transformed after propagating through a chiral sample (CS) into EP light. The resulting parallel ($E_{||}$) and perpendicular ($E_\perp$) electric field components with respect to the incident LP light (E_{ex}) are related to each other as $E_\perp/E_{||} = \delta + i\theta$. Here θ and δ are the ellipticity (CD) and optical rotation angle (ORD), respectively.[15]

In the ellipsometric method using LEP and REP beams as shown in Fig. 4b, the chiral signal ($E_\perp$) produced by the major-axis field of the EP (E_{ex}) is self-heterodyned with the internal LO phase-shifted by ±90° to $E_{||}$. Then, a polarizer (P) aligned perpendicular to E_{ex} eliminates the main background intensity ($|E_{||}|^2$) and allows detection of only the interference between $E_\perp$ and E_{LO}. For LEP and REP light, the measured intensities are

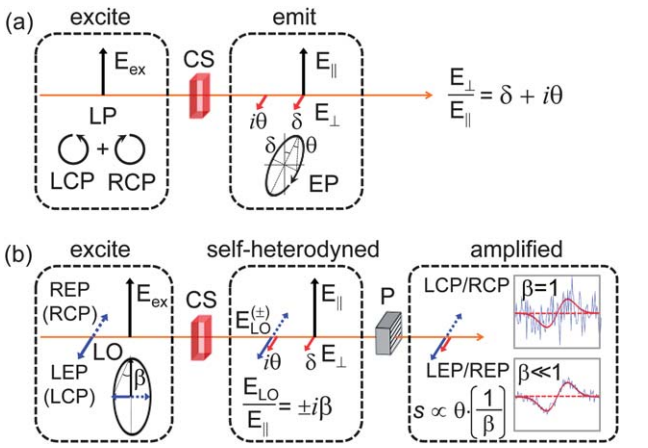

Fig. 4 (a) Relationship between parallel ($E_{||}$) and perpendicular ($E_\perp$) electric fields emitted by linearly polarized excitation. (b) Enhancement effect in self-heterodyne detection. CS: chiral sample; P: polarizer.

given as $I_\pm = |E_\perp + E_{LO}|^2 \approx |E_{LO}|^2 \pm 2\theta\ |E_{||}|\cdot|E_{LO}|$. Consequently, the chiral signal (s) in eqn (3) yields:

$$s = 4\theta \frac{|E_{||}||E_{LO}|}{|E_{LO}|^2} = 4\theta \cot\beta \cong \frac{4\theta}{\beta} \quad (5)$$

where the last approximate equality is obtained for small β ($=E_{LO}/E_{||}$), which corresponds to the ellipticity of the incident EP light. Note that $1/\beta$ is the enhancement factor as β approaches zero. The ORD signal ($\delta \propto n_L - n_R$), instead of the CD signal ($\theta \propto \varepsilon_L - \varepsilon_R$), can also be selectively measured by using rotated LP light where the LO is in- or out-of-phase to $E_{||}$. For LCP and RCP beams ($\beta = 1$), a large LO intensity (blue line in Fig. 4b) that equals $|E_{||}|^2$ results in a significant intensity fluctuation that overwhelms the chiral signal (red line). As the incident polarization becomes highly eccentric elliptical ($\beta \ll 1$), the LO contribution (background intensity) rapidly diminishes while the chiral signal is kept constant. Recently, it was shown that $s \propto |E_\perp^{EP}||B_\perp^{EP}|/|E_\perp^{EP}|^2$ (see eqn (3)), where $E_\perp^{EP}$ and $B_\perp^{EP}$ are the perpendicular (minor) components of the electric and magnetic field of the incident EP light.[18] As the ellipticity angle β decreases, the electric field energy density $|E_\perp^{EP}|^2$ decreases with a slight increase in $|B_\perp^{EP}|$, resulting in an amplification of s.

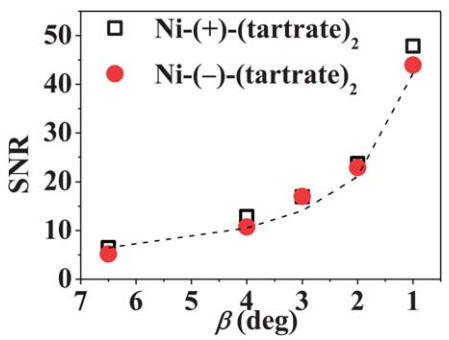

Fig. 5 Enhancement effects of self-heterodyne ORD signals monitored at 402 nm for (±)-Ni-(tartrate)$_2$.

Fig. 5 shows the ORD enhancement effect obtained by controlling the LO intensity (β) with rotated LP light. As estimated from the enhancement factor (dashed line), the ORD signal is amplified with $1/\beta$ and the SNR is increased accordingly. However, from our further studies (data not shown), we found that there are limits to enhancements in chiroptical signal measurements (similar to the case for optical enantioselectivity). The intrinsic limit occurs when the intensity of the chiral signal, $|E_\perp|^2$, exceeds the LO intensity, *i.e.*, $|E_\perp|^2 > E_\perp E_{LO}$. The practical limit is due to imperfect polarizers and/or dark noise of detectors. The maximum enhancement of the ORD signals achieved in the actual measurement is about 400. This allows a very weak ORD signal (<1 mdeg) to be detectable with a single optical pulse.[29]

The enhancement of g in eqn (4) demonstrated by the Cohen group, combined with the possibility of arbitrarily large enhancements to which their original theory alluded, generated much excitement in the field of optical enantioselectivity.[30] As they noted, the enhancement does not come from an increase in the optical chirality C, but rather arises from selectively positioning the chiral sample at the electric field node. This is because of the time-invariance of optical chirality for monochromatic fields, and because the EM energy density is contained in the denominator of the dissymmetry factor formula of eqn (4).

Let us explore this a little more in detail. Due to conservation of energy of the EM fields, the magnetic field energy is maximum at the electric field node, and hence must be included to correctly account for the enhancement. Accounting for this, the generalized formula for the dissymmetry enhancement for arbitrary fields is given by:[18]

$$\frac{g}{g_{CPL}} \cong \frac{cC}{2n\omega(U_e + \gamma U_b)} \quad (6)$$

where c is the speed of light, n is the average index of refraction, ω is the angular frequency, and U_e and U_b are the time-averaged electric and magnetic field energy densities, respectively. Here, $\gamma \propto$ (magnetic susceptibility/(electric polarizability) $\approx$ (10^{-6} to 10^{-4}), and hence is a property of the material used.

For the SWCF arrangement, eqn (6) can then be written as:[18]

$$\frac{g}{g_{CPL}} \cong \frac{1-R}{(1+R)(1+\gamma) + 2\sqrt{R}(\gamma-1)\cos(2kz)} \quad (7)$$

where $R = (E_{reflected}/E_{incident})^2$ is the reflectivity of the mirror used, k is the wave vector, and z is the position along the propagation direction of the fields. The dissymmetry factor is obtained by measuring the differential absorption of the 'left'- and 'right'-handed standing waves (created by an LCP incident light and an RCP light, respectively). For $R < 1$, these two SWCFs are either more left-handed or more right-handed than the other, thereby providing a non-zero dissymmetry factor. However, when $R = 1$ both SWCFs are the same, so we would expect $g = 0$.

The numerator $(1 - R)$ comes solely from the optical chirality C, and shows that C is constant in position and time, as expected. Hence, for fixed R an enhancement (g/g_{CPL}) can be obtained by minimizing the denominator in eqn (7), which is from the EM field energy density term ($U_e + \gamma U_b$) in eqn (6). Because of conservation of energy, this never becomes zero. However, it can be minimized when $U_e \approx 0$ since γ is so small, albeit at the cost of a weakened overall signal. In this limiting case of $\gamma \approx 0$, the enhancement factor, g/g_{CPL}, is approximately proportional to $|E_{SWCF}||B_{SWCF}|/|E_{SWCF}|^2$ so that, at the electric field node, the denominator approaches zero with finite numerator. This is essentially identical to the mechanism of chiroptical signal enhancements discussed above.

At the electric field node of the SWCF, *i.e.* when $\cos(2kz) = 1$, eqn (7) is plotted in Fig. 6. This plot shows the general shape of the enhancement as a function of R. We can see that the enhancement is finite ($\sim$18 for the material used) and that it goes to zero as R approaches 1, as expected. For a given material (hence constant γ), the maximum enhancement is fixed at $\sim 1/(2\sqrt{\gamma})$ and occurs when $U_e \approx \gamma U_b$. For realistic materials, this maximum is about 15 to 500. A search for materials with small $\sqrt{\gamma}$ is not necessarily practical, however, since the overall signal goes as γ (so the signal decreases faster than the gain in enhancement).[18]

Weak value measurements

The previously discussed chiroptical techniques have provided effective methods for enhancing the intrinsically small signals from chiral molecules. One chiroptical spectroscopy method in particular, ellipsometric detection in a quasi-null polarization geometry (Fig. 4b), has a straightforward connection to the vibrant subfield of quantum measurement known as "weak values".[10] The weak value was introduced in 1988 by Aharonov, Albert and Vaidman in order to explore time reversal symmetry in quantum mechanics. They showed that the result of a quantum measurement can yield a new value, similar to the eigenvalue of a quantum operator, but with unusual amplification behavior. After much debate concerning the interpretation of the weak value,[31] experimental results in metrology cemented this type of measurement as a *bona fide* protocol for the determination of photon polarization,[32] angstrom displacements,[8] optomechanical motion,[9] phase shifts,[33] spectroscopy,[34] a violation of Heisenberg's original uncertainty principle,[35] and even the quantum wave function itself.[36]

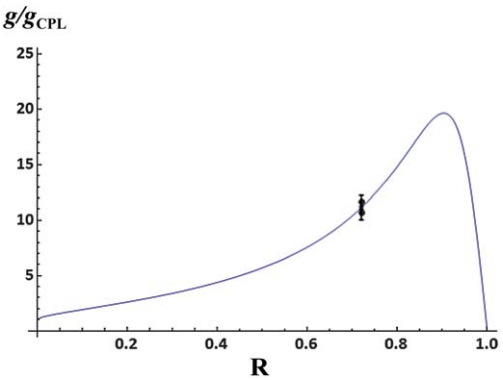

Fig. 6 Enhancement in dissymmetry factor *vs.* reflectivity R, for material used in ref. 23, with $\gamma = 6.5 \times 10^{-4}$ obtained by fitting to data. Dots w/ error bars are experimental data from the same source, for both enantiomers.

The weak value is often considered in the context of a two-state system (such as photon polarizations $\{|H\rangle, |V\rangle\}$) coupled to a continuous variable (such as position or momentum). To that end, consider a photon initially prepared in a polarization state $|\psi_i\rangle = a_H|H\rangle + a_V|V\rangle$ with a transverse spatial (momentum) wave function given by a Gaussian $\phi(x)$ [or $\phi(k)$]. The initial state is written as the product state $|\Psi\rangle = \int dx\, \phi(x)|x\rangle|\psi_i\rangle = \int dk\phi(k)|k\rangle|\psi_i\rangle$ in the position or momentum basis, respectively. Although the position/momentum and the polarization of the photon are initially separable (uncorrelated), the photon is passed through a device that entangles the two. This can be achieved, for instance, using a wedge of birefringent material as shown in Fig. 7, and modelled using a unitary operator $\hat{U} = \exp[-ik\hat{A}\hat{x}]$ that provides a small relative momentum shift k given by the polarization state. The operator $\hat{A}$ is known as the system operator and represents the connection between the photon polarization eigenstates and the continuous position variable x. For instance, in the case of Fig. 7, orthogonal polarizations are deflected by different amounts. The value of k is determined by the material properties and is assumed to be so small that the polarization eigenstates are not separated in either basis x or k. (Note that an analysis for a shift in x follows this same procedure.) Using a wedge of circular birefringent material, Ghosh and Fischer experimentally demonstrated that light can be split into left- and right-CPLs in a chiral liquid.[37] More recently, Pfeifer and Fischer showed that weak value amplified optical activity measurements can determine the sign of the splitting and thus the handedness of the optically active medium. They showed that angular beam separations of about 1 nanoradian could be measured accurately.[38]

The state of the photon is then post-selected on a final polarization state $|\psi_f\rangle = a'_H|H\rangle + a'_V|V\rangle$. For appropriate choices of the initial and final polarization states and a weak shift k, the resulting state of the photon is given by:

$$\langle\psi_f|\hat{U}|\Psi\rangle \approx \langle\psi_f|\psi_i\rangle \int dx\, e^{ikA_w x}\phi(x)|x\rangle \tag{8}$$

where the weak value is given by:

$$A_w = \frac{\left\langle \psi_f \middle| \hat{A} \middle| \psi_i \right\rangle}{\langle \psi_f | \psi_i \rangle} \tag{9}$$

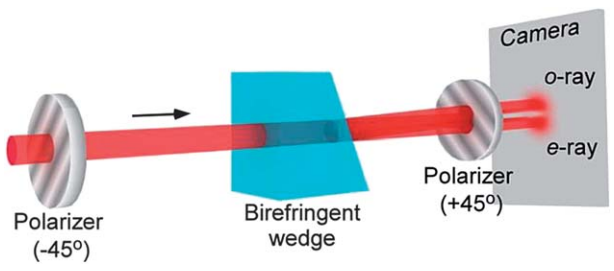

Fig. 7 An optical weak value experiment. A photon passes through a birefringent wedge placed between two polarizers. Orthogonal polarizations (*e.g.*, $|H\rangle$ and $|V\rangle$) experience opposite relative deflections $\pm k$ in the material due to linear birefringence of the material. The final position measurement of the photon gives information about the strength of k and therefore the birefringence of the chiral molecules.

The average position resulting from the pre- and post-selected state given by eqn (8) is shifted by the weak value A_w, which can be very large so long as $\langle\psi_f|\psi_i\rangle \ll 1$. Therefore, after the appropriate application of this pre- and post-selected protocol, the polarization states of the photon are well-separated in x, despite the fact that the birefringence of the material (represented by k here) may be extremely small. However, this amplification comes at the cost of reduced photon detection probability due to the small overlap of the initial and final polarization states. Despite the reduction in photon flux, the signal-to-noise ratio is often improved relative to standard measurement techniques.[39]

One may note that the weak value A_w can be complex in general. By consideration of eqn (8), for $A_w = \mathrm{Re}[A_w]$, this results in a shift of the momentum distribution given by the Fourier shift theorem. However, if $A_w = \mathrm{Im}[A_w]$, the shift is simply applied to the position distribution. Given these considerations, one therefore tailors the initial and final polarization states to obtain a real or imaginary weak value in order to produce the largest amplification.

For samples of chiral molecules that may exhibit both circular birefringence *and* circular dichroism, the analysis here has a straightforward extension where the operator $\hat{U}$ is no longer unitary owing to the polarization-dependent loss exhibited by the photons. In the case of the ellipsometric detection in a quasi-null polarization geometry, elliptically polarized pre- and post-selections are used and the continuous photon intensity is measured rather than the average photon position. In this case, the weak value formalism is equally applicable.

For the ellipsometric detection of chiroptical signals, we found that the transmitted electric field intensities, when the incident beams are (+) and (−) EP light, are:[11]

$$I_\pm = I_0 e^{2L\mathrm{Im}\left[A^\pm_{c,w}\right]} \sin^2\beta \tag{10}$$

where I_0 denotes the incident EP light intensity and β the ellipticity angle. The chiroptical weak value is given as:

$$A^\pm_{c,w} = \left(\rho \mp \frac{\Delta\rho}{2}\cot\beta\right) - i\left(\frac{\kappa}{2} \mp \frac{\Delta\kappa}{4}\cot\beta\right) \tag{11}$$

Here, L is the thickness of the solution sample and κ, ρ, $\Delta\kappa$, and $\Delta\rho$ are the absorption coefficient ($=\ln(10)\varepsilon c$), dispersion ($=\ln(10)2\pi n/\lambda$), circular dichroism (CD) ($=\ln(10)(\varepsilon_L - \varepsilon_R)c$), and circular birefringence ($=\ln(10)2\pi(n_L - n_R)/\lambda$), respectively, where ε, n, and λ are the decadic molar extinction coefficient, refractive index, and wavelength, respectively.

Then, the chiral signal s in eqn (3) can be obtained by inserting the weak value formulated $I_\pm$ in eqn (10) into the definition of s.[40] As can be seen in eqn (11), as the ellipticity angle β approaches zero, the real part of the chiroptical weak value in eqn (11) increases as $\cot\beta \sim 1/\beta$, though the enhancement factor is bounded by $|\cot\beta| < (\varepsilon_L + \varepsilon_R)/|\varepsilon_L - \varepsilon_R|$. Here, the price to pay is the loss of most of the transmitted photons passing through the second linear polarizer, which results in a weakened field intensity detected (proportional to $\sin^2\beta \sim \beta^2$ for small β). This decrease in measured intensity, for

the present quasi-null polarization detection scheme for chiroptical weak measurements, corresponds to the post-selection probability in quantum weak value measurements.

Conclusions

An overview of recent developments for enhancement methods in chiroptical spectroscopy, optical enantioselectivity, and weak value measurement has been provided. We can see that these techniques all have similarities, and some are actually the same effect.[11] All enhance intrinsically small signals, and all do so at the cost of large signal loss. Yet despite the reduced signal, for many cases the increased contrast (obtained by controlling the ratio of the post-selected magnetic to electric field amplitudes for some cases), and improved SNR are enough to be quite useful. There is already an effort to connect chiral fields and weak value measurements.[41] In the future, we look forward to continued improvements in these fields as ideas are shared and collaborations are made across disciplines.

Acknowledgements

This work was supported by the National Research Foundation of Korea (grant no.: 20090078897 and 20110020033) to MC and a KBSI grant (E33300) to HR. The experimental data presented here were measured using the UV-visible femtosecond laser system in KBSI. HR is grateful to Dr Deok-Soo Kim for his help in drawing a figure. JCH was supported by Army Research Office Grants no. W911 NF-12-1-0263 and no. W911-NF-09-0-01417. JSC was supported by an NSF IGERT Fellowship.

Notes and references

1 D. Fiedler, D. H. Leung, R. G. Bergman and K. N. Raymond, *Acc. Chem. Res.*, 2005, **38**, 349–358.
2 M. S. Taylor and E. N. Jacobsen, *Angew. Chem., Int. Ed.*, 2006, **45**, 1520–1543.
3 N. Berova, K. Nakanishi and R. W. Woody, *Circular dichroism: principles and applications*, Wiley-VCH, New York, Chichester, 2nd edn, 2000.
4 L. A. Nafie, *Vibrational optical activity: principles and applications*, Wiley, Syracuse, NY, 2011.
5 D. B. Amabilino, *Chirality at the nanoscale*, Wiley-VCH Verlag GmbH & Co. KGaA, Weinheim, 2009.
6 C. Gautier and T. Bürgi, *J. Am. Chem. Soc.*, 2006, **128**, 11079–11087.
7 K. C. Hannah and B. A. Armitage, *Acc. Chem. Res.*, 2004, **37**, 845–853.
8 O. Hosten and P. Kwiat, *Science*, 2008, **319**, 787.
9 P. B. Dixon, D. J. Starling, A. N. Jordan and J. C. Howell, *Phys. Rev. Lett.*, 2009, **102**, 173601.
10 Y. Aharonov, D. Z. Albert and L. Vaidman, *Phys. Rev. Lett.*, 1988, **60**, 1351.
11 M. Cho, *Phys. Rev. A*, 2013, submitted.
12 J. W. Lewis, R. F. Tilton, C. M. Einterz, S. J. Milder, I. D. Kuntz and D. S. Kliger, *J. Phys. Chem.*, 1985, **89**, 289; R. A. Goldbeck, D. B. Kim-Shapiro and D. S. Kliger, *Annu. Rev. Phys. Chem.*, 1997, **48**, 453.
13 H. Rhee, Y.-G. June, J.-S. Lee, K.-K. Lee, J.-H. Ha, Z. H. Kim, S.-J. Jeon and M. Cho, *Nature*, 2009, **458**, 310–313.
14 I. Eom, S. H. Ahn, H. Rhee and M. Cho, *Phys. Rev. Lett.*, 2012, **108**, 103901.
15 H. Rhee, I. Eom, S.-H. Ahn and M. Cho, *Chem. Soc. Rev.*, 2012, **41**, 4457–4466.
16 M. Cho, *Two-dimensional optical spectroscopy*, CRC Press, Boca Raton, 2009.
17 Y. Tang and A. E. Cohen, *Phys. Rev. Lett.*, 2010, **104**, 163901.
18 J. S. Choi and M. Cho, *Phys. Rev. A*, 2012, **86**, 063834.
19 D. M. Lipkin, *J. Math. Phys.*, 1964, **5**, 696–700.
20 T. W. B. Kibble, *J. Math. Phys.*, 1965, **6**, 1022–1026; D. J. Candlin, *Nuovo Cimento*, 1965, **37**, 1390–1395; D. M. Fradkin, *J. Math. Phys.*, 1965, **6**, 879–890.
21 R. P. Cameron, S. M. Barnett and A. M. Yao, *New J. Phys.*, 2012, **14**, 053050; S. M. Barnett, R. P. Cameron and A. M. Yao, *Phys. Rev. A*, 2012, **86**, 013845.
22 J. W. Lewis, R. A. Goldbeck, D. S. Kliger, X. Xie, R. C. Dunn and J. D. Simon, *J. Phys. Chem.*, 1992, **96**, 5243–5254.
23 J. Helbing and M. Bonmarin, *J. Chem. Phys.*, 2009, **131**, 174507.
24 I. Eom, S.-H. Ahn, H. Rhee and M. Cho, *Opt. Express*, 2011, **19**, 10017–10028.
25 H. Rhee, J.-H. Choi and M. Cho, *Acc. Chem. Res.*, 2010, **43**, 1527–1536; H. Rhee, S.-S. Kim, S.-J. Jeon and M. Cho, *ChemPhysChem*, 2009, **10**, 2209–2211.
26 L. Lepetit, G. Cheriaux and M. Joffre, *J. Opt. Soc. Am. B*, 1995, **12**, 2467–2474.
27 L. Barron, *Molecular light scattering and optical activity*, Cambridge University Press, Cambridge, UK, 2nd edn, 2004.
28 Y. Tang and A. E. Cohen, *Science*, 2011, **332**, 333.
29 Since $E_{\perp}$ rarely exceeds E_{LO} in most cases, the enhancement mainly depends on the practical limit. In our case, the detectable level was determined by the standard deviation (0.8 mdeg) of ORD signals obtained with 3000 pulses at $\beta = 0.005$ and $E_{\perp}/E_{LO}$ ~0.1.
30 A. G. Smart, *Phys. Today*, 2011, **64**, 16.
31 I. M. Duck, P. M. Stevenson and E. C. G. Sudarshan, *Phys. Rev. D: Part. Fields*, 1989, **40**, 2112; A. Cho, *Science*, 2011, **333**, 690.
32 N. W. M. Ritchie, J. G. Story and R. G. Hulet, *Phys. Rev. Lett.*, 1991, **66**, 1107; G. J. Pryde, J. L. O'Brien, A. G. White, T. C. Ralph and H. M. Wiseman, *Phys. Rev. Lett.*, 2005, **94**, 220405.
33 D. J. Starling, P. B. Dixon, N. S. Williams, A. N. Jordan and J. C. Howell, *Phys. Rev. A*, 2010, **82**, 011802; N. Brunner and C. Simon, *Phys. Rev. Lett.*, 2010, **105**, 010405.
34 D. J. Starling, P. B. Dixon, A. N. Jordan and J. C. Howell, *Phys. Rev. A*, 2010, **82**, 063822.
35 L. A. Rozema, A. Darabi, D. H. Mahler, A. Hayat, Y. Soudagar and A. M. Steinberg, *Phys. Rev. Lett.*, 2012, **109**, 100404.
36 J. S. Lundeen, B. Sutherland, A. Patel, C. Stewart and C. Bamber, *Nature*, 2011, **474**, 188; S. Kocsis, B. Braverman, S. Ravets, M. J. Stevens, R. P. Mirin, L. K. Shalm and A. M. Steinberg, *Science*, 2011, **332**, 1170.

37 A. Ghosh and P. Fischer, *Phys. Rev. Lett.*, 2006, **97**, 173002.
38 M. Pfeifer and P. Fischer, *Opt. Express*, 2011, **19**, 16508–16517.
39 D. J. Starling, P. B. Dixon, A. N. Jordan and J. C. Howell, *Phys. Rev. A*, 2009, **80**, 041803 (R).
40 The relationship between $\Delta\kappa(\Delta\rho)$ in eqn (11) and $\theta(\delta)$ in Fig. 4 and eqn (5) is $\Delta\kappa = 4\theta/L$ ($\Delta\rho = 2\ln(10)\delta/L$).
41 Y. Gorodetski, K. Y. Bliokh, B. Stein, C. Genet, N. Shitrit, V. Kleiner, E. Hasman and T. W. Ebbesen, *Phys. Rev. Lett.*, 2012, **109**, 013901; K. Y. Bliokh, A. Y. Bekshaev and F. Nori, *New J. Phys.*, 2013, **15**, 033026.